AUSTRALASIAN JOURNAL OF COMBINATORICS
Volume **81(2)** (2021), Pages 319–333

Color-induced subgraphs dual to Hamilton cycles of embedded cubic graphs

SARAH-MARIE BELCASTRO*

Mathematical Staircase, Inc.
Holyoke, MA 01040
U.S.A.

Abstract

We consider properly edge 3-colored cellularly embedded cubic graphs and their dual Grünbaum-colored triangulations. The collection of edges of a single color induces a matching in the cubic graph and, in the dual triangulation, a *color-induced subgraph (CISG)*. We examine the structure of CISGs that correspond to Hamilton cycles in embedded cubic graphs. Unsurprisingly, the CISG structure depends on the embedding surface. For all surfaces, we characterize CISG structure in triangulations when the dual cubic graph has a Hamilton cycle. Conversely, for the projective plane and the torus, we give conditions on CISGs that reveal that a Hamilton cycle must exist in the dual cubic graph.

1 Introduction and summary

We begin with the basics. A *Hamilton cycle* of a graph is a cycle that includes all vertices of the graph. A *cubic* graph is 3-regular and a *proper edge 3-coloring* assigns three colors to edges such that no two incident edges receive the same color. Any Hamilton cycle of a cubic graph can be edge 2-colored, leaving the remaining edges to be assigned a third color.

A graph G is *cellularly embedded* on a surface S when $S \setminus G$ is a collection of topological disks, each of which defines a *face* of the embedding. Associated to a cellularly embedded graph G is its *topological dual* G^*, which is another graph embedded on S such that each vertex of G^* corresponds to a face of G embedded on S, and an edge joins two vertices of G^* exactly when the two corresponding faces of G embedded on S share an edge. (A multiple edge of G^* corresponds to two faces of G that meet at more than one edge.) Note that the topological dual of a topological dual is the original embedding.

* Also at: Smith College, Northampton, MA 01063, U.S.A.

ISSN: 2202-3518

The topological dual of an embedded cubic graph is a *triangulation*, and the topological dual of a proper edge 3-coloring is a *Grünbaum coloring*, where each triangle's edges use all three colors.

Note that while every embedded cubic graph is dual to a triangulation, not every cubic graph has a proper edge 3-coloring, from which it follows that not every embedded triangulation has a Grünbaum coloring. We will only consider embedded cubic graphs for which there exists a proper edge 3-coloring and, likewise, Grünbaum-colored triangulations dual to those embedded cubic graphs. This is a reasonable restriction because while there are infinite families of embedded triangulations without Grünbaum colorings on orientable surfaces of genus at least five [6] and nonorientable surfaces of genus at least two ([3], [8]), there are more classes of triangulations that have Grünbaum colorings: most toroidal triangulations [1], all even-degree triangulations of sufficiently low genus or high representativity [7], and projective-planar triangulations with all but two (adjacent) vertices of even degree [5].

Usually an *induced subgraph* of a graph G results from selecting a subset U of vertices and including all edges of G that connect vertices of U. A *color-induced* subgraph (or *CISG*) is induced by edges of a single color in a Grünbaum coloring; this includes vertices of G incident to any edge of a given color. For convenience in notation, we refer to a properly edge 3-colored cubic graph cellularly embedded on a surface S as C, and refer to its dual Grünbaum colored triangulation as T. If C has a Hamilton cycle, we denote it as H. We label the edge colors of both C and T as c_1, c_2, and c_3, so that a generic pair of colors will be c_i, c_j and a generic color will be c_k, with $i, j, k \in \{1, 2, 3\}$. A CISG of T induced by the edges of color c_i will be denoted G_i.

Our results are as follows. In Section 2 we show that certain CISG structures on projective planar and toroidal triangulations indicate the presence of Hamilton cycles in the dual cubic graphs. Conversely, in Section 3, given the existence of a Hamilton cycle of a cubic graph on any surface, we derive the structure of a CISG in the corresponding triangulation. We finish in Section 4 with corollaries for low-genus surfaces, extensions to theorems from Section 2, and examples showing that CISG structure is not enough to determine existence of a Hamilton cycle for higher-genus surfaces.

2 CISG structures implying the existence of Hamilton cycles

We identify CISG structures on the plane, projective plane, and torus that imply the existence of a Hamilton cycle in the dual cubic graph. Note that every planar triangulation has a Grünbaum coloring, and every planar cubic graph has a proper edge 3-coloring, by the Four Color Theorem, Tait's Theorem, and duality.

Theorem 2.1. *For a planar cubic graph C and dual triangulation T, there exists a c_i-c_j Hamilton cycle H in C if and only if G_k in T forms two trees.*

For a given planar triangulation, there are generally multiple Grünbaum colorings,

often all Kempe equivalent. Thus, even if a particular Grünbaum coloring does not have a two-trees CISG, there may still be a Hamilton cycle in the underlying dual cubic graph (associated to a different edge coloring that *does* have a two-trees CISG).

Although Theorem 2.1 follows from a result in [11], we present a proof that builds intuition for later theorems. The following proof is similar in structure to that of Lemma 5 of [2].

Proof of Theorem 2.1. First assume that C has a Hamilton cycle H. The interior of H is a disk subdivided by a matching, all edges of which have color c_k. Thus G_k, the dual of the interior embedding, is a tree: Note that contraction of an edge in G_k corresponds to deletion of the corresponding c_k edge in C. This edge of C separated two faces of the embedding, so its removal reduces the number of vertices of G_k by one. Because every c_k edge of C is incident on both ends to the exterior of the disk bounded by H, no c_k edge of C can be monofacial (even after all other c_k edges are deleted) and therefore by induction G_k can be contracted to a single point (dual to an empty disk). This means it is acyclic and connected, and thus a tree. See Figure 1 for examples of this process. Likewise, the exterior of H is a disk subdivided by a

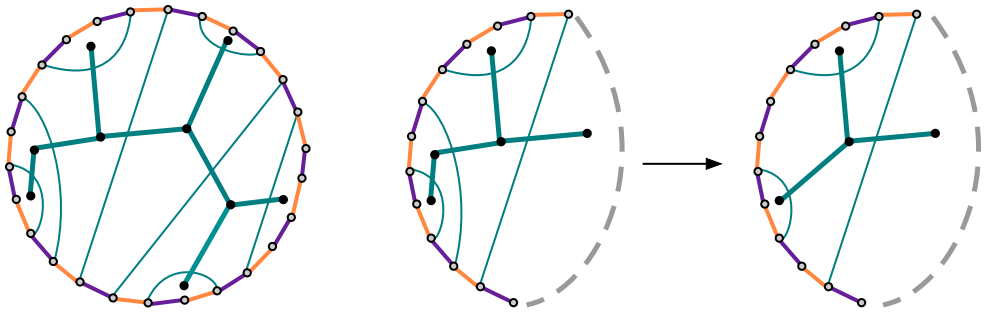

Figure 1: At left, a purple-orange cycle with an interior teal-colored matching and dual teal-colored CISG component; at right, the contraction of a tree edge and corresponding deletion of a matching edge.

c_k-colored matching, and so its dual is also a tree. Therefore the c_k CISG consists of two trees.

Now for the converse: We know the c_i, c_j edges in C form a collection of disjoint cycles $\{Z_t\}$. Suppose that G_k is two trees, but C does not have a Hamilton cycle. The collection $\{Z_t\}$ must contain more than one cycle, and elements of the collection are joined by c_k edges in C. Now we have cases depending on the planar embedding of C.

Case 1: Some Z_r lie(s) inside some Z_s. Consider the c_k edges singly incident to the exterior of Z_r and inside of Z_s. (See Figure 2(left) for an example.) The corresponding c_k edges in T form a cycle homotopic to Z_r. This contradicts the fact that G_k is acyclic.

Case 2: No Z_r lies inside any Z_s. Consider the c_k edges singly incident to and outside of one of the $Z_s \in \{Z_t\}$. The corresponding c_k edges in T form a cycle homotopic

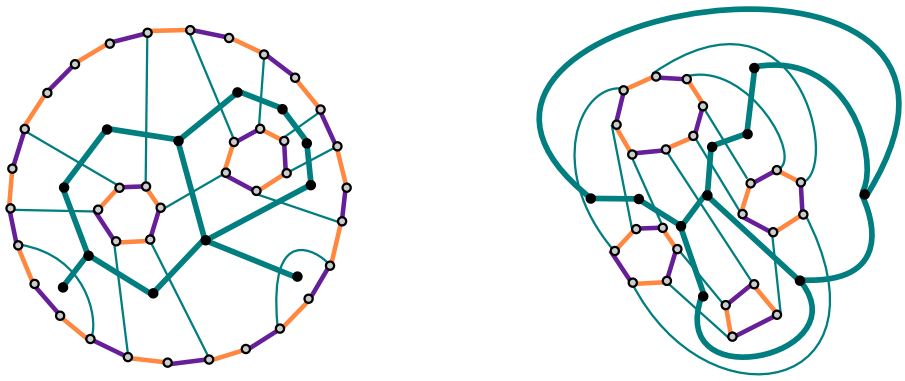

Figure 2: At left, the component of a teal-colored CISG corresponding to two Z_r inside some Z_s; at right, the component of a teal-colored CISG corresponding to a collection of $\{Z_t\}$, none of which lies inside any other.

to Z_s. (See Figure 2(right) for an example.) This contradicts the fact that G_k is acyclic. □

We now move on to the case of the projective plane.

Theorem 2.2. *If the c_k CISG of a Grünbaum coloring of a projective-planar triangulation T is a spanning tree, then C has a c_i-c_j Hamilton cycle.*

Proof. Suppose not. That is, suppose G_k is a spanning tree but C has multiple (disjoint) c_i-c_j cycles. At most one such cycle can be noncontractible, as any two noncontractible loops on a projective plane must intersect. Thus at least one c_i-c_j cycle Z_t must be contractible, which means it bounds a disk and thus is a Jordan curve. All c_k edges inside Z_t are separated from the c_k edges outside Z_t, which means that in T the dual c_k edges—the c_k CISG—must have at least two components. This is a contradiction to G_k's connectedness. □

Finally, we give a criterion for the torus.

Theorem 2.3. *If the c_k-induced subgraph of a toroidal triangulation T is connected and spans T, then there exists a c_i-c_j Hamilton cycle in C.*

Note that it is possible to have a connected c_k CISG in T corresponding to two (or more) c_i-c_j cycles in C, at least one of which surrounds an isolated vertex of T. Figure 3 shows such a toroidal triangulation with two connected non-spanning CISGs.

Proof of Theorem 2.3. Suppose that G_k is connected and that the set $\{Z_r\}$ of disjoint c_i-c_j cycles in C has at least two elements. The Z_r are connected by c_k edges. There are two possibilities:
Case 1: At least one of the Z_r is contractible. Here, the Jordan Curve Theorem applies and one of the Z_r cycles has an interior separated from its exterior. Thus G_k

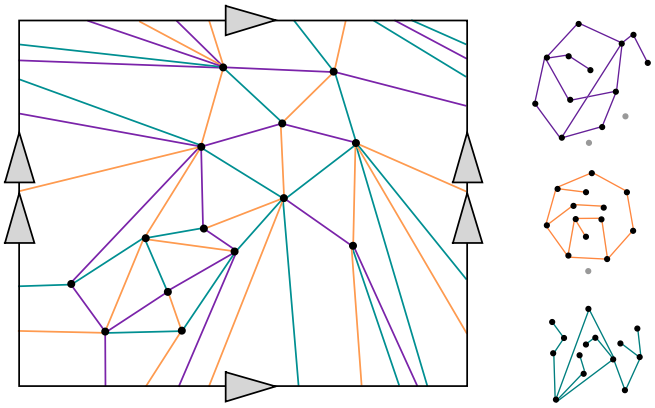

Figure 3: The fourth partial Grünbaum coloring of the $(5, 4)$ embedding of K_6 on the torus (see [1]), completed to a Grünbaum colored triangulation; the CISGs are displayed separately. Isolated vertices (that are not part of the CISGs) are shown in grey.

must have at least two components, which contradicts the fact that G_k is connected. Case 2: None of the Z_r are contractible. Any two disjoint noncontractible c_i-c_j cycles on the torus are homotopically equivalent, and thus their removal separates the torus into two disjoint annuli. There must be edges of G_k in each of these annuli (or else T is not cellularly embedded) with no vertices of T on the boundary, and thus G_k must have multiple components—again, a contradiction. □

3 The structure of CISGs in the presence of a Hamilton cycle

Shelton and Gottlieb [4] prove that on the sphere, a Grünbaum coloring of a triangulation has all CISGs connected if and only if the triangulation has all vertices of even degree. They also give an example of an even triangulation on the torus for which there exists a Grünbaum coloring such that one of the CISGs has two components. Interestingly, in their example G_1 is a cycle, and the c_2, c_3 edges in C form a Hamilton cycle $H_{2,3}$; the same is true for G_2 and $H_{1,3}$. (G_3 is a pair of cycles and the c_2, c_2 edges do not form a Hamilton cycle.) Both $H_{2,3}$ and $H_{1,3}$ are noncontractible. This, together with Theorem 2.1, suggests that there is a relationship between the form of G_i and whether $H_{j,k}$ is contractible. The focus of this section is on discerning that relationship.

Lemma 3.1 (with Mike Albertson and Ruth Haas)**.** *If there exists a contractible c_i-c_j Hamilton cycle $H_{i,j}$ in C on the surface S, then the c_k-induced subgraph of T consists of two components, at least one of which is a tree.*

Proof. First note that a contractible cycle is also a surface-separating cycle, so that the interior of the cycle is a disk. Because $H_{i,j}$ is contractible, we may use the Jordan

Curve theorem to note that the interior of $H_{i,j}$ corresponds to a tree component of G_k by the same reasoning as in the start of the proof of Theorem 2.1. Let the tree component of G_k be R. Now suppose that $G_k \setminus R$, the remainder of G_k, is not connected. Note that all edges external to $H_{i,j}$ are of color c_k, and that each vertex of $G_k \setminus R$ corresponds to a face in C. Traveling around the outside of $H_{i,j}$ from face to face, we must find some face of C that shares c_k edges with two different components of $G_k \setminus R$. But this is a contradiction, as all c_k edges of a given face are part of the same component of G_k. □

We can make stronger statements.

Theorem 3.2. *If there exists a contractible c_i-c_j Hamilton cycle $H_{i,j}$ in C on the surface S, then the c_k-induced subgraph of T consists of two components; one is a tree and the other is contractible to a bouquet of loops of the same cardinality of a minimal set of generators for $\pi_1(S)$.*

To provide some intuition for this theorem, we give an example on the torus.

Example 3.3. Figure 4 shows a cubic graph embedded on the torus with a contractible Hamilton cycle. The two-component teal CISG is also shown in bold. Ob-

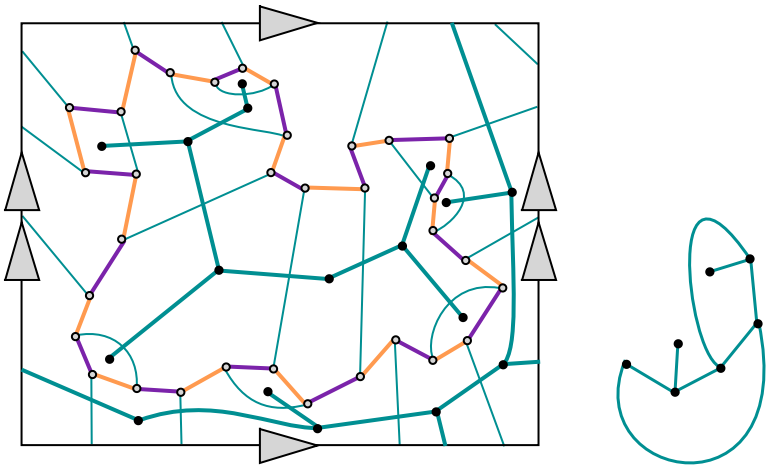

Figure 4: A cubic graph embedded on the torus with a contractible Hamilton cycle in bold, and the two-component teal CISG in bold. At right, the component not interior to the Hamilton cycle is shown separately.

serve that the component outside the disk of the Hamilton cycle contains two cycles, each of which is parallel to a pair of polygon edges. Viewed in the plane, it is clear that this component is contractible to a bouquet of two loops.

Theorem 3.4. *If there exists a noncontractible and non-surface-separating c_i-c_j Hamilton cycle $H_{i,j}$ in C on the surface S, then the c_k-induced subgraph of T is connected and contractible to a bouquet of loops, one fewer in number than the cardinality of a minimal set of generators for $\pi_1(S)$.*

Again, we provide some intuition via an example on the torus.

Example 3.5. Figure 5 shows the cubic graph dual to a Grünbaum colored triangulation of the torus (a completion to a triangulation of the fourth partial Grünbaum coloring of the $(5, 4)$ embedding of K_6; see [1]). The purple-orange Hamilton cycle is shown in bold, as is the corresponding teal CISG. Despite the seeming complexity

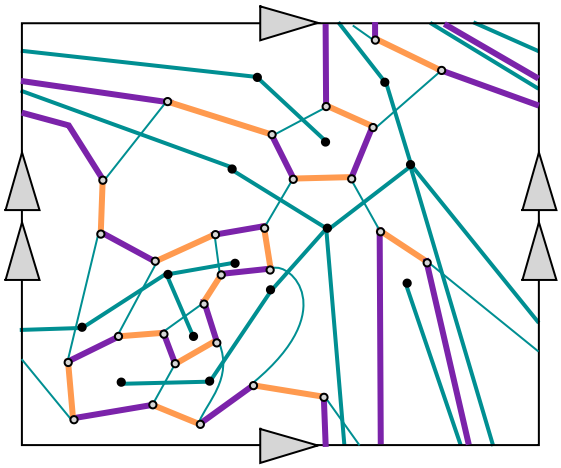

Figure 5: A cubic graph on the torus with noncontractible Hamilton cycle in bold and corresponding CISG in bold.

of the Hamilton cycle, slicing along it leaves a (weirdly shaped) cylinder. The teal CISG has a single cycle that wraps once around this cylinder and tree appendages that reach into pockets on the boundaries of the cylinder. See Figure 6.

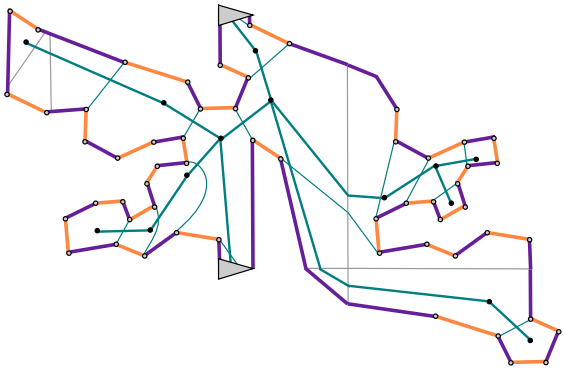

Figure 6: A cut-and-paste redrawing of Figure 5.

Theorem 3.6. *If there exists a noncontractible surface-separating c_i-c_j Hamilton cycle $H_{i,j}$ in C on the surface S, then the c_k-induced subgraph of T consists of two components, each contractible to a bouquet of loops that together have the cardinality of a minimal set of generators for $\pi_1(S)$.*

Here, the simplest example is on the Klein bottle.

Example 3.7. Figure 7 shows the cubic graph dual to a partial Grünbaum coloring of the embedding of $C_3 + C_5$ on the Klein bottle (see [1]), completed to a Grünbaum colored triangulation. The purple-orange Hamilton cycle is shown in bold, as is the corresponding two-component teal CISG. It is not immediately obvious that the

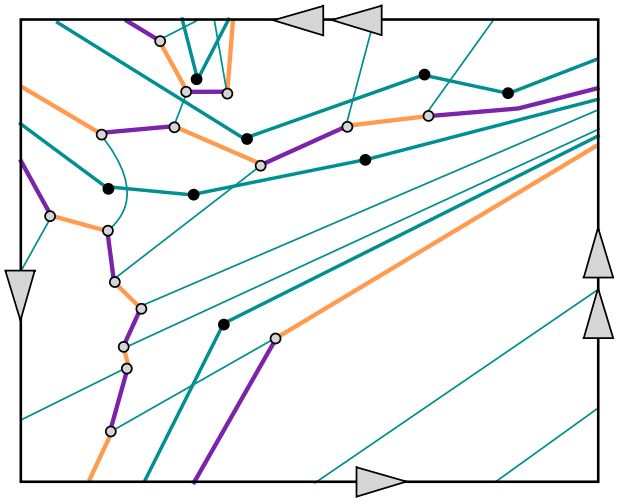

Figure 7: A cubic graph on the Klein bottle with surface-separating Hamilton cycle in bold and corresponding two-component CISG in bold.

Hamilton cycle is surface-separating, but using the polygon representation, cutting along the Hamilton cycle, and carefully pasting the results will reveal that this is the case; see Figure 8. It is easier to see that the corresponding CISG is the union of a 3-cycle and a 5-cycle. The Hamilton cycle separates the Klein bottle into two Möbius bands, and each teal CISG component wraps around one of those Möbius bands.

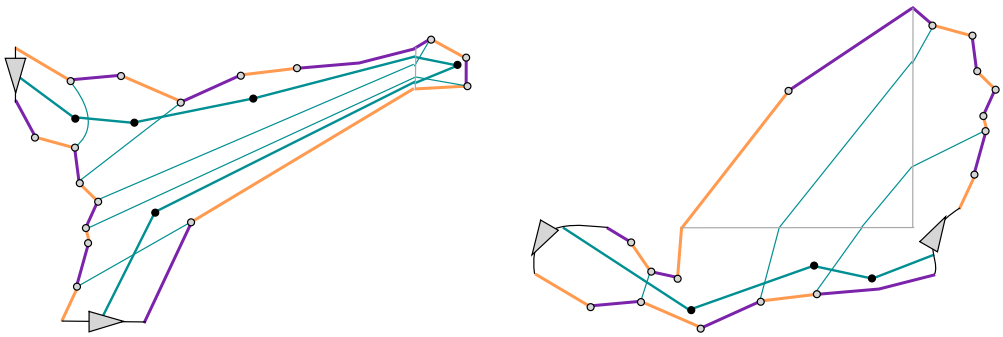

Figure 8: A cut-and-paste redrawing of Figure 7 that shows the Hamilton cycle is surface-separating.

Before proceeding with proofs of Theorems 3.2–3.6, we need two facts:

Theorem 3.8 (well known; see e.g. [10], Ch. 2)**.** *Two compact topological surfaces are homeomorphic if and only if they have the same Euler characteristics, number of boundary curves, and orientability type (orientable or nonorientable).*

In particular, knowing both $\chi(S)$ and the number of boundary curves of a surface S, there are at most two possibilities for the topological type of S, each of which has the same number of generators for the fundamental group $\pi_1(S)$. Note that given a normal-form polygonal representation of S, we can choose a base point on the interior of the polygon and construct a bouquet of loops, each of which passes through one of the marked polygon edges, that forms a generating set for $\pi_1(S)$.

Lemma 3.9. *Given any simple noncontractible (and non-surface-separating) loop on a surface S without boundary, cutting along that loop produces a surface S' with boundary and $\chi(S') = \chi(S)$.*

Proof. Consider a triangulation of S and a simple noncontractible non-surface-separating loop γ. This triangulation can be refined such that edges and vertices of the refined triangulation T' cover γ. Note that $\chi(S) = v(T') - e(T') + f(T')$ and that there are exactly k vertices and k edges of T' on γ. Cutting along γ to obtain S', we see that $\chi(S') = (v(T') + k) - (e(T') + k) + f(T') = \chi(S)$. □

Observation. In the orientable case, cutting along a noncontractible loop γ adds two boundary components while the number of handles goes down by one. In the nonorientable case, there are two possibilities; cutting along a 2-sided noncontractible loop adds two boundary components and reduces the number of handles by one, and cutting along a 1-sided noncontractible loop adds one boundary component while removing a crosscap. Thus in all cases $\pi_1(S')$ has one less generator than $\pi_1(S)$. Recall that if S is orientable, so is S'. In contrast, if S is nonorientable then S' may be either orientable or nonorientable. Using the normal-form polygonal representation, a nonorientable surface has (up to homotopy/homeomorphism) one 1-sided loop, so for S nonorientable, if γ is 1-sided then S' is orientable and vice-versa.

Proof of Theorem 3.2. Suppose there is a contractible Hamilton cycle $H_{i,j}$ in C embedded on S, with the disc bounded by $H_{i,j}$ denoted D. First, we note that by Lemma 3.1 there are exactly two components of the c_k CISG, one of which is a tree. Consider the non-tree component N of the c_k CISG. Its dual matching M in C is embedded on $S' = S \setminus D$. The edges of M define faces of S', where each face is bounded by edges from M alternating with sequences of edges (boundary segments) from $H_{i,j}$. Every edge in M is either incident to two different $H_{i,j}$ boundary segments, or is incident to one $H_{i,j}$ boundary segment twice. Note that those faces of M on S' that have a single boundary segment from M (and a single boundary segment from $H_{i,j}$) correspond to leaves in N.

An edge of N corresponding to a non-monofacial edge of M can be contracted without changing the topological structure of N, and the corresponding edge in M

can be deleted. Repeating and completing this process leaves a bouquet of loops B that is topologically equivalent to N. None of these loops is contractible, as otherwise some edge of M would have an endpoint not on $H_{i,j}$. On a reduced polygon representation of S', there is a one-to-one correspondence between loops of B and pairs of arrowed polygon edges: Every pair of arrowed polygon edges must have a loop crossing it, or else there is a noncontractible path within the face of C corresponding to the single vertex of B. This is not possible because every face of C was a disk before edge-deletions, and no monofacial edges were deleted. Moreover, no pair of arrowed polygon edges has two loops crossing it, as this would form a 2-sided face and therefore some edge of M would have an endpoint not on $H_{i,j}$.

Therefore there are the same number of loops as generators of $\pi_1(S')$. Because S was a surface without boundary and removing a disk is equivalent to adding a single puncture, $\pi_1(S') \cong \pi_1(S)$ and so they have the same number of generators. □

Proof of Theorem 3.4. Suppose there is a noncontractible and non-surface-separating Hamilton cycle $H_{i,j}$ in C embedded on S. By cutting along $H_{i,j}$, consider G_k embedded on $S' = S \setminus H_{i,j}$, a surface with boundary consisting of edges of $H_{i,j}$.

We claim that G_k has only one component. Otherwise, we proceed similarly to the proof of Lemma 3.1; there must be some face of C that shares c_k edges with two different components of G_k, which is again a contradiction.

Next, we claim that G_k is contractible to a bouquet of loops B; as in Theorem 3.2, we successively contract edges of G_k corresponding to non-monofacial edges of M. Also following the proof of Theorem 3.2 we claim that none of the resulting loops is contractible and that there is a one-to-one correspondence between loops of B and pairs of arrowed polygon edges. Again, there are the same number of loops as generators of $\pi_1(S')$.

By Lemma 3.9, S' is a surface with $\chi(S') = \chi(S)$ and either one (if $H_{i,j}$ is nonorientable) or two (if $H_{i,j}$ is orientable) boundaries. Now by Theorem 3.8, we know the topological type of S' because we know $\chi(S')$, the number of boundaries, and the orientability type. By the observation following Lemma 3.9, the genus goes down by one from S to S', so we know that $\pi_1(S)$ has one more generator than $\pi_1(S')$ has. □

Proof of Theorem 3.6. Suppose there is a noncontractible surface-separating Hamilton cycle $H_{i,j}$ in C embedded on S. Here we note that G_k has exactly two components. There are at least two components because each edge in G_k is in one of the two surfaces S_1, S_2 joined by the surface-separating loop $H_{i,j}$. Each of these surfaces is topologically equivalent to some surface minus a disk, with $\chi(S_1) + \chi(S_2) = \chi(S)$. (Recall that each of S_1, S_2 has a boundary.) Moreover, in terms of the polygon representation, cutting along a surface-separating loop simply produces two smaller polygons (each with a boundary), so the number of generators of $\pi_1(S)$ is the sum of the numbers of generators of $\pi_1(S_1)$ and $\pi_1(S_2)$.

By applying the proof of Theorem 3.2 to S_1, S_2, the result follows. □

4 Consequences and counterexamples

We first state explicitly the consequences of Theorems 3.2–3.6 for low-genus surfaces. In this section, we use the phrase *edge-contractible to a cycle* to describe a subgraph that after a sequence of edge contractions can be simplified to a cycle, to distinguish this from the term *contractible*, used here to indicate a curve that is homotopically trivial.

Note that by Lemma 3.9 and Theorem 3.8, cutting along any noncontractible simple loop on the torus leaves a cylinder. (There are no noncontractible surface-separating loops on the torus.)

Corollary 4.1. *Suppose that C is embedded on the torus with Hamilton cycle $H_{i,j}$.*

- *If $H_{i,j}$ is contractible, then G_k, the c_k CISG of T, consists of two components, one a tree and the other contractible to a bouquet of two loops.*
- *If $H_{i,j}$ is noncontractible, then G_k is edge-contractible to a cycle.*

Removing a disk from the projective plane leaves a Möbius band; because any noncontractible simple loop on the projective plane P is homotopic to the generator of $\pi_1(P)$, cutting along such a loop leaves a disk. (There are no noncontractible surface-separating loops on the projective plane.)

Corollary 4.2. *Suppose that C is embedded on the projective plane with Hamilton cycle $H_{i,j}$.*

- *If $H_{i,j}$ is contractible, then G_k, the c_k CISG of T, consists of two components, one a tree and the other edge-contractible to a cycle.*
- *If $H_{i,j}$ is noncontractible, then G_k consists of a single tree.*

The Klein bottle is the connected sum of two projective planes, so cutting along a noncontractible surface-separating loop produces two Möbius bands. On the other hand, cutting along a noncontractible non-surface-separating loop may result (depending on the choice of loop) in either a Möbius band or a cylinder.

Corollary 4.3. *Suppose that C is embedded on the Klein bottle with Hamilton cycle $H_{i,j}$.*

- *If $H_{i,j}$ is contractible, then G_k, the c_k CISG of T, consists of two components, one a tree and the other contractible to a bouquet of two loops.*
- *If $H_{i,j}$ is noncontractible and non-surface-separating, then G_k is edge-contractible to a cycle.*
- *If $H_{i,j}$ is noncontractible and surface-separating, then G_k consists of two components, each edge-contractible to a cycle.*

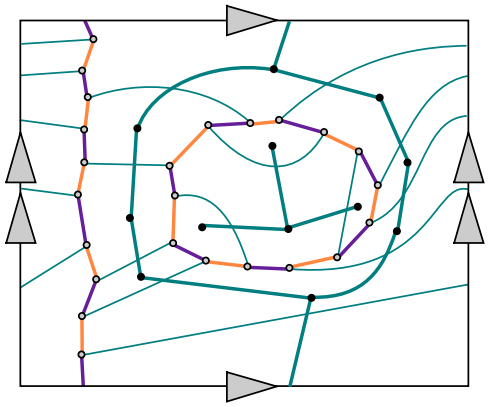

Figure 9: A cubic graph on the torus that gives a counterexample to the converse of Lemma 3.1.

Example 4.4. Unsurprisingly, the converse of Lemma 3.1 does not hold; Figure 9 shows a cubic graph on the torus where G_k has two components, one of which is a tree, and there are two c_i-c_j cycles.

On the other hand, we can use Lemma 3.1 to strengthen Theorem 2.3.

Corollary 4.5. *If the c_k-induced subgraph of a toroidal triangulation T is connected and spans T, then the associated c_i-c_j Hamilton cycle in C is not contractible.*

However, Theorem 2.3 does not extend to the 2-holed torus, nor does the converse of Corollary 4.3 hold. In general, the appropriate converses of Theorems 3.2–3.6 do not hold, as seen in the following example.

Example 4.6. There exist triangulations of the 2-holed torus with

- a c_k-CISG that includes all vertices and has two components, one a tree and one contractible to a bouquet of four loops, but the c_i-c_j edges of the dual cubic graph form two cycles (see Figure 10);
- a connected c_k-CISG that includes all vertices, and in particular is contractible to a bouquet of three loops, but the c_i-c_j edges of the dual cubic graph form two cycles (see Figure 11); and
- a c_k-CISG that includes all vertices and has two components, each contractible to a bouquet of two loops, but the c_i-c_j edges of the dual cubic graph form two cycles (see Figure 12);

and triangulations of the Klein bottle with

- a c_k-CISG that includes all vertices and has two components, one a tree and one contractible to a bouquet of two loops, but the c_i-c_j edges of the dual cubic graph form two cycles (see Figure 10);

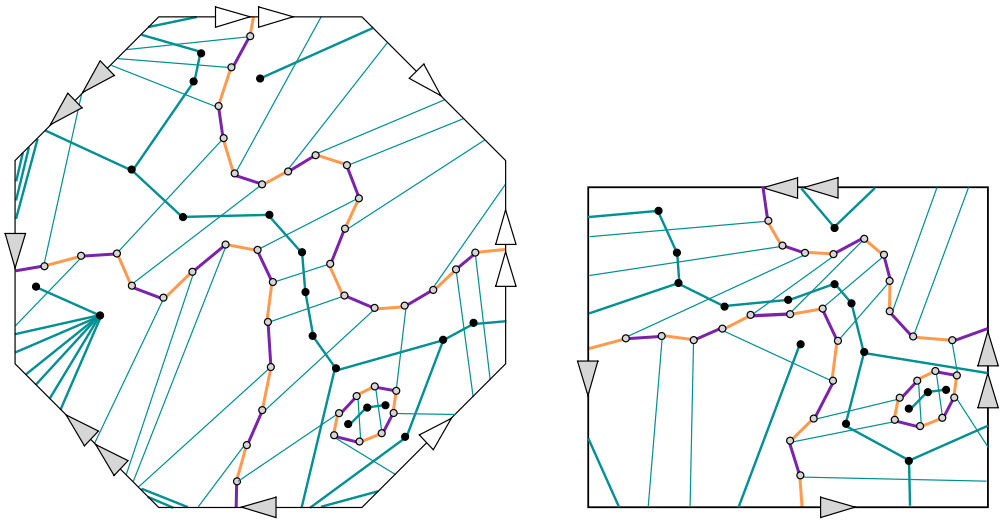

Figure 10: A triangulation of the two-holed torus (left) and a triangulation of the Klein bottle (right) that each shows a counterexample to an appropriate converse of Theorem 3.2.

- a connected c_k-CISG that includes all vertices, and in particular is edge-contractible to a cycle, but the c_i-c_j edges of the dual cubic graph form two cycles (see Figure 11); and
- a c_k-CISG that includes all vertices and has two components, each edge-contractible to a cycle, but the c_i-c_j edges of the dual cubic graph form two cycles (see Figure 12).

Finally, part of the proof of Theorem 2.1 extends to other surfaces.

Corollary 4.7. *If there exists a contractible path enclosing a collection* $\{Z_t\}$ *of contractible* c_i-c_j *cycles in* C *then there is a* c_k *cycle in* T.

We can also observe that in this situation there may also be a noncontractible c_k cycle in T between two noncontractible Z_t.

5 Conclusion and further work

In this paper, we have given conditions (for some surfaces) on CISG structure that mean the dual cubic graph must have a Hamilton cycle, and analyzed the CISG structure that results from the existence of a Hamilton cycle on any surface. Some of our results can be seen as specializations of results in [9]; however, our proofs are substantively different. In particular, [9] proves theorems of the form "A k-regular graph embedded on a surface has a Hamilton cycle if and only if the corresponding CISG complement has [a given form] *and* the corresponding CISGs form a facial

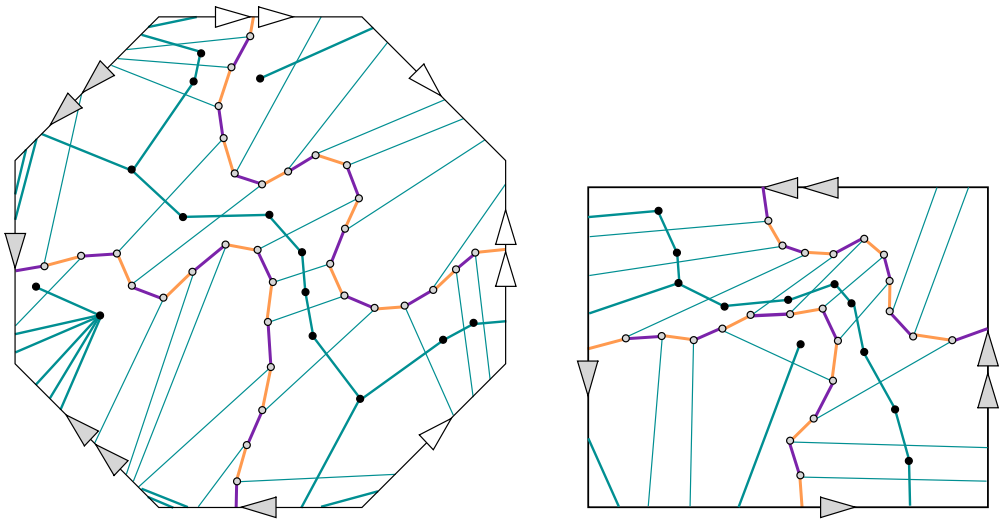

Figure 11: A triangulation of the two-holed torus (left) and a triangulation of the Klein bottle (right) that each shows a counterexample to an appropriate converse of Theorem 3.4.

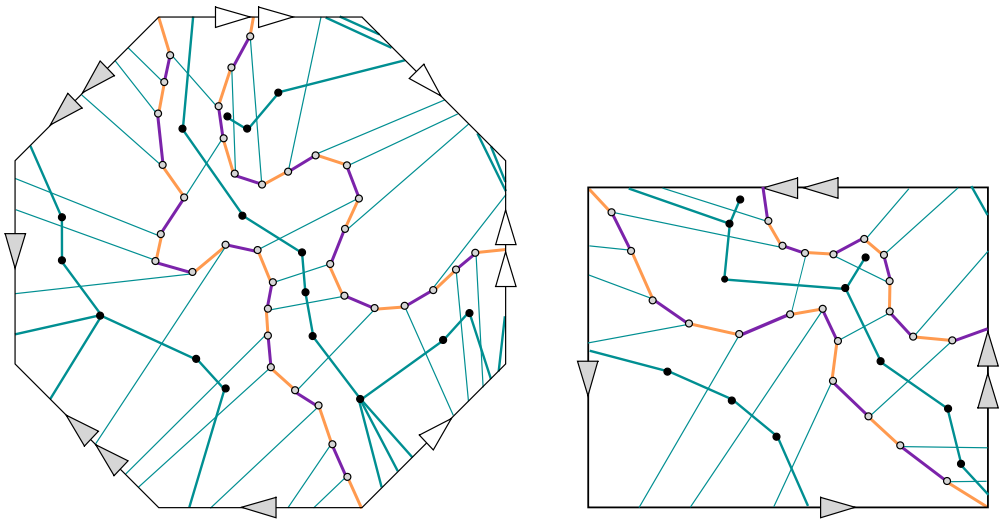

Figure 12: A triangulation of the two-holed torus (left) and a triangulation of the Klein bottle (right) that each shows a counterexample to an appropriate converse of Theorem 3.6.

Hamilton cycle." That is, these results achieve the combination of necessity and sufficiency by adding a substantial restriction.

A clear direction for further work is the question: Are there other conditions we could impose in addition to the prescribed CISG structure in order to force a Hamilton cycle? That is, what would it take to rule out our counterexamples to Theorems 3.2–3.6?

Acknowledgements

Thanks to Hannah Alpert and Josh Greene for useful conversations about the exposition of the topology background, and thanks to Mike Albertson and Ruth Haas for discussions of these problems many years ago.

References

[1] M. O. Albertson, H. Alpert, s-m. belcastro and R. Haas, Grünbaum colorings of toroidal triangulations, *J. Graph Theory* **63** (1) (2010), 68–81.

[2] H. Alt, M. S. Payne, J. M. Schmidt and D. R. Wood, Thoughts on Barnette's Conjecture, *Australas. J. Combin.* **64** (2016), 354–365.

[3] s-m. belcastro, Small snarks and 6-chromatic triangulations on the Klein bottle, *Australas. J. Combin.* **65** (3) (2016), 232–250.

[4] E. Gottlieb and K. Shelton, Color-induced subgraphs of Grünbaum colorings of triangulations of the sphere, *Australas. J. Combin.* **30** (2004), 183–192.

[5] M. Kasai, N. Matsumoto and A. Nakamoto, Grünbaum colorings of triangulations on the projective plane, *Discret. Appl. Math.* **215** (2016), 155–163.

[6] M. Kochol, Polyhedral embeddings of snarks in orientable surfaces, *Proc. Amer. Math. Soc.* **137** (2009), 1613–1619.

[7] M. Kotrbčík, N. Matsumoto, B. Mohar, A. Nakamoto, K. Noguchi, K. Ozek and A. Vodopivec, Grünbaum colorings of even triangulations on surfaces, *J. Graph Theory* **87** (4) (2018), 475–491.

[8] W. Liu and Y. Chen, Polyhedral Embeddings of Snarks with Arbitrary Nonorientable Genera, *Electron. J. Combin.* **19** (3) (2012), #P14.

[9] D. Maity and A. K. Upadhyay, Hamiltonian cycles in polyhedral maps, *Proc. Math. Sci.* **127** (4) (2017), 737–751.

[10] W. S. Massey, *Algebraic Topology: An Introduction* (GTM 56), Springer, New York, 1967.

[11] S. Stein, B-sets and planar maps, *Pacific J. Math.* **37** (1) (1971), 217–224.

(Received 8 Oct 2020; revised 30 May 2021)